Journal of Engineering and Applied Research (JEAR)

National University of Skill

Winter & Spring 2026, Vol. 3, No. 1, p. 69-87

Journal Homepage: https://jear.tvu.ac.ir

:10.48301/jear.2025.496460.1057

Proposing an Exact Solution and Order Study of Solution for Added Mass and Added Damping Coefficients of Oscillating Circular Cylinder

Amir Basirparsa[1], Mohammad Ali Kazemi [2]*

[1]Mechanical Engineering Department, Hamedan University of Technology, Hamedan, Iran.

[2]Department of Mechanical Engineering, Technical and Vocational University (TVU), Tehran, Iran.

ARTICLE INFO

Article Type:
Original Research

Received: 2025.01.05
Revised: 2025.01.31
Accepted: 2025.03.16

Keyword:
Added mass
Added damping
Exact solution
Order study

***Corresponding Author:**
Mohammad Ali Kazemi
Email: m-kazemi@tvu.ac.ir

ABSTRACT

The present work concerns the analytical solution to estimate of added mass and damping coefficient of a large surface-piercing and bottom-mounted vertical circular cylinder undergoing an oscillating motion. For added mass coefficient, numerical results are presented for various order of solution (an order study). These results show that forth order of solution is agreeable generally. Some numerical results are compared with the previously published data. The comparison shows good agreement. In addition, effects of geometric parameters on the added mass and damping are investigated. Existence of the singular nature causes considerable difficulties in computing the added mass for higher frequencies than the corresponding computation of the damping coefficient. This is encountered when we compute infinite number of eigenvalues. Comparison with previous work indicates good agreement over a range of frequencies the added mass and damping coefficient are plotted along with the actual analytical solutions and performing of the solution until higher order cause that solution procedure be very long.

©2024 the authors. Published by National University of Skill, Tehran, Iran. This article is an open-access article distributed under the terms and conditions of the Creative Commons Attribution-Noncommercial 4.0 International (CC BY-NC 4.0 license) (https://creativecommons.org/licenses/by-nc/4.0/).

E-ISSN: 3060-6357

1) Introduction

Axisymmetric cylinders are used in many ocean engineering applications such as drilling rigs, buoys and instrumentation platforms because of their simplicity of construction. In fluid mechanics, added mass or virtual mass is the inertia added to a system because an accelerating or decelerating body must move (or deflect) some volume of surrounding fluid as it moves through it. Hydrodynamic coefficients for simple vertical circular cylinders at finite depth were reported earlier by Sabuncu and Calisal [1]. A comprehensive set of theoretical added masses and wave damping data for a floating circular cylinder in finite-depth water is presented by Yeung [2, 3] . The usual methods of calculation for such geometries obtained on finite element solutions by [4] or on the solution of integral equations. Bai [5] calculated added mass coefficients for horizontal and vertical cylinders.

The loads associated with the motion of the structure are examples of one category of hydrodynamic loads. Those loads are present due to various factors, for example, wave excitation, ice impact, or ground acceleration. If the structure is large enough compared with the length of the water particle excursion, flow separation will not occur, the drag force component is negligible, and the flow tield can be treated by classical methods of potential theory. The problem can be further simplified by linearizing the governing equations with the help of the additional assumption of small amplitude motions. Then an added mass and a damping coefficient, which correspond to components that are in phase with the acceleration and velocity of the structure, respectively, can be used to express the resulting hydrodynamic forces. The added mass is associated with a mass of fluid that is accelerated by the structure due to the generation of surface waves. Of the two approaches available, the numerical approach can be applied to compute hydrodynamic coefficients for a large structure of arbitrary geometries using a boundary integral method, a boundary element method, or a finite element method. To predict the added mass and damping coefficient of bodies oscillating in a free surface, there exists a variety of elaborate numerical techniques in the literature. Faltinsen and Michelsen [6] and Fenton [7] used the traditional wave source distribution method (Green's function method) [8]. Bai and Yeung' and Che and Mei [9] used the finite element variation method. Rahman [10] present a good account of the theoretical development. Second-order theory applicable to a finite depth case has been done by Rahman and Chakravartty [11]. Two more papers by Rahman [12] have appeared in the literature concerning the second-order diffraction theory. Drobyshevski [13] applied the methodology of matched asymptotic expansions to obtain analytical solutions [14] for hydrodynamic coefficients of a circular cylindrical platform in extremely shallow water.

Rahman and Bhatta [15] described an analytical solution to the velocity potential that governs the linear radiation problem. Two numerical methods have been reviewed to predict hydrodynamic loadings on the submerged cylinders advancing in waves in by Wu [16]. Also a computation of added mass and damping coefficients due to a heaving cylinder has been done by Bhatta [17]. A theoretical model of an added mass representation for a flexible cylinder vibrating in a fluid medium was presented by Han and Xu [18]. Bonion et al [19].presented a multiphase model for the added-mass phase to have a different temperature and density than the particle and bulk-fluid phases, and to account for mass transfer from the particle phase to the added-mass phase. Also, Sanchez et al [20]. presented a model, which allows for a more precise representation of the added mass terms in the potential flow equations, combining low computational cost and accurate modeling.

The present paper considers the added mass and damping coefficient for a vertical surface-piercing circular cylinder extending to the seabed and undergoing horizontal oscillations. An analytical solution using an eigenfunction expansion is obtained for the linear radiation problem. Attention is given to the low-frequency and high-frequency behavior of the hydrodynamic coefficients. Theoretical predictions are presented in graphical forms and compared with the other analytical work collected by Rahman and Bhatta [15]. In addition an order study for solution of added mass is presented.

2) Formulation of the Problem

As shown in Fig. 1 (see to Ref [15]), the circular cylinder of radius a with a vertical surface-piercing that extends to the seabed in water of depth h (Fig. 1). This cylinder undergoes a sinusoidal, unidirectional motion with displacement $\zeta(t)$ and velocity $u(t)$ given by (see to Ref [15])

$$\zeta(t) = \frac{iU}{\omega} e^{-i\omega t}, \tag{1}$$

$$u(t) = Ue^{-i\omega t}. \tag{2}$$

The flow assumed to be irrotational and consider an incompressible flow. The flow can be described by a complex velocity potential ϕ that satisfies the Laplace equation within the fluid region (see to Ref [15])

$$\nabla^2\phi = 0, \tag{3}$$

$$\frac{\partial^2\phi}{\partial r^2} + \frac{1}{r}\frac{\partial\phi}{\partial r} + \frac{1}{r^2}\frac{\partial^2\phi}{\partial\theta^2} + \frac{\partial^2\phi}{\partial z^2} = 0. \tag{4}$$

This velocity potential is subject to kinematic and dynamic free surface boundary conditions to bottom boundary condition, to body surface boundary condition, and to a far field radiation condition. The boundary conditions for this case are as follows:

Kinematic dynamic free surface boundary conditions

$$\frac{\partial\phi}{\partial z} = \frac{\partial\eta}{\partial t} \quad \text{at} \quad z = 0, \tag{5}$$

dynamic free surface boundary conditions

$$\eta = -\frac{1}{g}(\frac{\partial \phi}{\partial t}) \quad \text{at} \quad z = 0, \tag{6}$$

therefore

$$\frac{\partial^2 \phi}{\partial r^2} + g\,\frac{\partial \phi}{\partial z} = 0 \quad \text{at} \quad z = 0, \tag{7}$$

bottom boundary condition

$$\frac{\partial \phi}{\partial z} = 0 \quad \text{at} \quad z = -h, \tag{8}$$

body surface boundary condition□

$$\frac{\partial \phi}{\partial r} = V_n \qquad \text{at} \quad r = a, \; -h < z < \eta, \tag{9}$$

far field radiation condition

$$\lim_{r \to \infty} \sqrt{r}\,(\frac{\partial \phi}{\partial r} - ik\,\phi) = 0, \tag{10}$$

In this equations, η is the complex free surface elevation above the still water level produced due to the oscillation of the cylinder and V_n is the velocity of the cylinder surface that is normal to the surface. It could be wrote

$$V_n = U\,\cos(\theta) e^{-i\,\omega t}. \tag{11}$$

3) Solution procedure

In this section Eq. (4) with its boundary conditions is solved by the separation of variables method. The governing partial differential equation has been transformed into a system of ordinary differential equations. The final solution can be expressed as a product of the solutions of the ordinary differential equations, each of which is an equation containing only one of the independent variables. Thus the product solution can be written as

$$\phi(r,\theta,z,t) = R(r)\Theta(\theta)Z(z)T(t). \tag{12}$$

The velocity potential ϕ may be expressed in terms of an eigenfunction expansion that satisfies Laplace's equation and all relevant boundary conditions stated above except that on the body surface. In addition we can assume $T(t)$ to be proportional to $e^{-i\,\omega t}$. If we replace Eq. (12) into Eq. (4), then

$$R''(r)\Theta(\theta)Z(z)T(t)+\frac{1}{r}R'(r)\Theta(\theta)Z(z)T(t)+$$
$$\frac{1}{r^2}R(r)\Theta''(\theta)Z(z)T(t)+R(r)\Theta(\theta)Z''(z)T(t)=0, \tag{13}$$

division two side of this equation to $R(r)\Theta(\theta)Z(z)T(t)$

$$\frac{R''(r)}{R(r)}+\frac{1}{r}\frac{R'(r)}{R(r)}+\frac{1}{r^2}\frac{\Theta''(\theta)}{\Theta(\theta)}+\frac{Z''(z)}{Z(z)}=0, \tag{14}$$

where a prime denotes differentiation with respect to the argument. Introducing separation constants m and k, we can write this equation as

$$\frac{R''(r)}{R(r)}+\frac{1}{r}\frac{R'(r)}{R(r)}-\frac{m^2}{r^2}+k^2=0, \tag{15}$$

$$\Theta''(\theta)+m^2\Theta(\theta)=0, \tag{16}$$

$$Z''(z)-k^2Z(z)=0, \tag{17}$$

For obtaining a physical solution must $m^2\geq 0$. Various conditions for k will be investigated.

3.1. Propagating mode of solutions $(\boldsymbol{k}^2>0)$:

For $\boldsymbol{k}^2>0$, solutions of ordinary differential equations (15-17) could be shown simply as

$$R(r)=C_1J_m(kr)+C_2Y_m(kr), \tag{18}$$

$$\Theta(\theta)=C_3Cos(m\theta)+C_4Sin(m\theta), \tag{19}$$

$$Z(z)=C_5\cosh(kz)+C_6\sinh(kz). \tag{20}$$

Therefore

$$\phi_1(r,\theta,z,t)=A\cos(m\theta)[B\cosh(kz)+C\sinh(kz)]H_m^{1}(kr)e^{-i\omega t} \tag{21}$$

where A, B and C are arbitrary constants. It is to be noted here that this form of solution satisfies the far field radiation condition stated by Eq. (10). From Eqs. (8), (21)

$$C = B\,\frac{\sinh(kh)}{\cosh(kh)}. \tag{22}$$

Therefore

$$Z(z) = B\,\frac{\cosh(k(z+h))}{\cosh(kh)}. \tag{23}$$

Then, the free surface boundary condition (6) gives rise to the condition

$$\omega^2 = gk\,\tanh(kh). \tag{24}$$

Which is known as the linear dispersion relation. Here k is the wavenumber and can be regarded as the eigenvalue. The transcendental equation (24) has only one eigenvalue and hence corresponding to the eigenvalue k, there is only one eigenfunction $Z(z)$. It will be clear from the evanescent mode of solutions that we are going to consider next that the solution of $Z-$differential equation forms an orthogonal set of eigenfunctions $\{Z(z)\},\ n = 0,1,2,...,$ defined in the interval $-h \le z \le 0.$ From the orthonormal property of the eigenfunctions, we can write

$$\begin{aligned}\int_{-h}^{0} Z^2(z)dz = 1, \ \Rightarrow \int_{-h}^{0} B^2\,\frac{\cosh^2(k(z+h))}{\cosh^2(kh)}dz = 1,\\ \Rightarrow B^2\int_{-h}^{0}\cosh^2(k(z+h))dz = \cosh^2(kh),\end{aligned} \tag{25}$$

.

so that

$$B = \frac{\cosh(kh)}{C_0}, \tag{26}$$

where

$$C_0 = \sqrt{\frac{h}{2}\left(1+\frac{\sinh(2kh)}{2kh}\right)}, \tag{27}$$

thereupon

$$\phi_1(r,\theta,z,t)=\alpha_{0m}\cos(m\theta)f_0(z)H_m{}^1(kr)e^{-i\omega t}, \tag{28}$$

where

$$f_0(z)=\frac{\cosh(k(z+h))}{C_0} \tag{29}$$

and α_{0m} is the unknown complex coefficient.

3.2. Evanescent mode of solutions $(\boldsymbol{k}^2<0)$:

For $\boldsymbol{k}^2>0,$ solutions of ordinary differential equations (15-17) could be shown simply as

$$R(r)=C_1J_m(-ikr)+C_2Y_m(-ikr), \tag{30}$$

$$\Theta(\theta)=C_3Cos(m\theta)+C_4Sin(m\theta), \tag{31}$$

$$Z(z)=C_5\cos(kz)+C_6Sin(kz). \tag{32}$$

In this case, a general solution for the evanescent mode can be obtained by a suitable combination of all these particular solutions:

$$\phi_2(r,\theta,z,t)=A\cos(m\theta)[B\cos(k_nz)+C\sin(k_nz)]K_m{}^1(k_nr)e^{-i\omega t} \tag{33}$$

where A,B and C are arbitrary constants. It is to be noted that recent equation satisfies the far field radiation condition. Using the bottom boundary condition (8), we obtain

$$Z(z)=B\cos(k_nz)+C\sin(k_nz)=B\,\frac{\cos(k_n(z+h))}{\cos(k_nh)}. \tag{34}$$

Thus using condition (7), the dispersion relation in this case becomes

$$\omega^2=-gk_n\tan(k_nh), \tag{35}$$

This equation has an infinite number of roots, in other words, an infinite number of eigenvalues $k_n,\ n=1,2,3,...$ corresponding to each eigenvalue, there is an eigknfunction $Z_n(z)$. It can easily be shown that the set of functions $\{Z(z)\},\ n=0,1,2,...,$ (0 includes the propagating mode) is an orthogonal set defined in the interval $-h \le z \le 0$. Thus as before an orthonormal set will be given by using the property,

$$\int_{-h}^{0} Z_n^{\,2}(z)dz = 1, \tag{36}$$

so that

$$B = \frac{\cosh(k_n h)}{C_n}, \tag{37}$$

where

$$C_n = \sqrt{\frac{h}{2}(1+\frac{\sinh(2k_n h)}{2k_n h})}, \tag{38}$$

thereupon

$$\phi_2(r,\theta,z,t) = \sum_{n=1}^{\infty}[\alpha_{nm} K_m(k_n r) f_n(z)]\cos(m\theta)e^{-i\omega t}, \tag{39}$$

where

$$f_n(z) = \frac{\cos(k_n(z+h))}{C_n} \tag{40}$$

and α_{nm} is the unknown complex coefficient.

3.3. Added mass and added damping:

Total velocity potential is obtained by superposing all the solutions given by Eqs. (33) and (39) for each m

$$\phi(r,\theta,z,t) = \sum_{m=0}^{\infty}[\phi_m \cos(m\theta)]e^{-i\omega t}, \tag{41}$$

where

$$\phi_m = \alpha_{0m} H_m^{\,1}(kr) f_0(z) + \sum_{n=1}^{\infty}[\alpha_{nm} K_m(k_n r) f_n(z)]. \tag{42}$$

When α_{0m} and α_{nm} are initially unknown complex coefficients. From Eqs. (9), (11), and (41), we obtain

$$\sum_{m=0}^{\infty}[k\,\alpha_{0m}\,H^{1}{}_{m}{}'(ka)f_0(z)+\sum_{n=1}^{\infty}[k_n\alpha_{nm}K'_m(k_na)f_n(z)]]\cos(m\theta)]=U\cos(\theta). \quad (43)$$

For $m=1$:

$$k\,\alpha_{01}\,H^{1}{}_{1}{}'(ka)f_0(z)+\sum_{n=1}^{\infty}[k_n\alpha_{n1}K'_1(k_na)f_n(z)]=U. \quad (44)$$

Set of functions $f_n(z),\ n=1,2,3,...$ is an orthonormal set defined in $-h\le z\le 0$. Therefore, to obtain the unknown complex coefficients α_{01} and α_{n1}, we multiply both sides of Eq. (44) by $f_j(z)$ for $j=0,1,2,3,...$ and integrate with respect to z over $(-h,0)$, which yields

$$\int_{-h}^{0}[k\,\alpha_{01}\,H^{1}{}_{1}{}'(ka)f_0(z)+\sum_{n=1}^{\infty}[k_n\alpha_{n1}K'_1(k_na)f_n(z)]]\,f_j(z)dz=\int_{-h}^{0}Uf_j(z)dz. \quad (45)$$

For $j=0$:

$$k\,\alpha_{01}\,H^{1}{}_{1}{}'(ka)=U\int_{-h}^{0}f_0(z)dz, \quad (46)$$

and for $j=n$:

$$k_n\alpha_{n1}K_1'(k_na)=U\int_{-h}^{0}f_n(z)dz, \quad (47)$$

therefore

$$\alpha_{01}=\frac{U}{kH^{1}{}_{1}{}'(ka)}\int_{-h}^{0}f_0(z)dz=\frac{U}{kH^{1}{}_{1}{}'(ka)}\frac{\sinh(kh)}{kC_0} \quad (48)$$

and

$$\alpha_{n1}=\frac{U}{k_nK_1'(k_na)}\frac{\sin(k_nh)}{k_nC_n},n=1,2,3,.... \quad (49)$$

The linearized unsteady form of Bernoulli's equation is

$$\rho \frac{\partial \phi}{\partial t} + P = 0, \tag{50}$$

thus

$$P(r, \theta, z, t) = -\rho \frac{\partial \phi}{\partial t} = i\,\omega\rho\phi(r, \theta, z, t). \tag{51}$$

The total horizontal hydrodynamic radiated force on the cylinder is given by

$$\begin{aligned} F &= \int_{-h}^{0}\int_{0}^{2\pi} -P(a, \theta, z, t)\cos(\theta) a\, d\theta dz = -i\,\omega\rho a \int_{-h}^{0}\int_{0}^{2\pi} \phi(a, \theta, z, t)\cos(\theta)\, d\theta dz \\ &= -i\,\omega\rho a\pi[\alpha_{01} H_1^1(ka) c_0 + \sum_{n=1}^{\infty}(\alpha_{n1} K_1(k_n a) c_n)] e^{-i\omega t}. \end{aligned} \tag{52}$$

Where

$$c_0 = \frac{\sinh(kh)}{kC_0}, \quad c_n = \frac{\sin(k_n h)}{kC_n}. \tag{53}$$

This radiated force F can be decomposed into components in phase with the velocity and the acceleration of the structure in the following manner

$$F = -(\mu \frac{\partial^2 \zeta(t)}{\partial t^2} + \lambda \frac{\partial \zeta(t)}{\partial t}), \tag{54}$$

where μ and λ are the total added mass and damping coefficients, respectively, and are considered real. Now from Eqs. (1), (52), and (54) we get

$$\mu\omega + i\,\lambda = -\omega\rho a\pi(\frac{H^1{}_1(ka)}{kH^1{}_1{}'(ka)} c_0{}^2 + \sum_{n=1}^{\infty}[\frac{K_1(k_n a)}{k_n K_1{}'(k_n a)} c_n{}^2]). \tag{55}$$

The dimensionless added mass and damping coefficient can be obtained by equating the real and imaginary parts of the following equation:

$$\frac{\mu}{\rho a^3} + i\, \frac{\lambda}{\rho a^3 \omega} = -[Y], \tag{56}$$

where

$$Y = \pi(\frac{kc_0{}^2}{(ka)^2} \frac{H^1{}_1(ka)}{H^1{}_1{}'(ka)} + \sum_{n=1}^{\infty}[\frac{k_n c_n{}^2}{(k_n a)^2} \frac{K_1(k_n a)}{K_1'(k_n a)} c_n{}^2]). \tag{57}$$

Thus the corresponding dimensionless damping coefficient and added mass could be wrote respectively

$$\frac{\lambda}{\rho a^3 \omega} = -\mathrm{Im}[Y\ ] = -\pi \left(\frac{k{c_0}^2}{(ka)^2} \mathrm{Im}\frac{{H^1}_1(ka)}{{H^1}_1{}'(ka)}\right), \tag{58}$$

$$\frac{\mu}{\rho a^3} = -\mathrm{Re}[Y\ ] = -\pi \left(\frac{k{c_0}^2}{(ka)^2} \mathrm{Re}\frac{{H^1}_1(ka)}{{H^1}_1{}'(ka)} + \sum_{n=1}^{\infty}\left[\frac{k_n{c_n}^2}{(k_na)^2}\frac{K_1(k_na)}{K_1{}'(k_na)}\right]\right), \tag{59}$$

where $k{c_0}^2$ is a function of kh and $k_n{c_n}^2$ are functions of $k_nh.$ These two coefficients are numerically evaluated and presented in graphical form. In the following section we will discuss the asymptotic behavior of these two coefficients for high and low frequency waves.

4) Properties of Hankel functions

Hankel functions are the mathematical functions, suitable for both symbolic and numerical manipulation. ${H_m}^1(x)$ is given by $J_m(x)+iY_m(x)$ and ${H_m}^2(x)$ is given by $J_m(x)-iY_m(x).$ ${H_m}^1(x)$ has a branch cut discontinuity in the complex z plane running from $-\infty$ to $0.$ For certain special arguments, Hankel functions automatically evaluates to exact values and can be evaluated to arbitrary numerical precision.

5) Comparisons and verification

It is worth citing that for $h/a = 3.57, h/a = 5.0$ and our problem is comparable with Rahman and Bhatta [15] To verify the accuracy of our results, the present results are compared in Figs. 2-5 with recent reference and are found to be in good agreement.

6) Results and Discussion

The specific formulas used for the calculation of added mass and damping coefficients (Eqs. (58), (59)) are investigated in this section physically and mathematically. The required routines for the calculation of Bessel and Hankel functions and solution of linear equations are obtained by Mathematica software. For higher values of ka calculations of added mass coefficient are very difficult. This difficulty is primarily due to the singular nature of the equation $ka\tanh(kh) = -k_na\tan(k_nh)$ for a given ka and $kh.$

Fig. 6 shows analytical values computed for added damping coefficients as a function of ka for various values of $h/a.$ It is clear that the analytical curves increase sharply as ka increases for small values of ka for all $h/a.$ For intermediate values of $ka,$ these curves start decreasing. It has been found that the decreasing rate is very slow for large values of ka and approaches zero in infinity. Fig. 7 illustrates the dimensionless added mass as functions of ka for different values of h/a. It is interesting, Existence of both maximum and minimum points of this curves in a short distance.

For study of solution's order of added mass coefficient, Figs. 8-11 are presented. These figures show analytical solution of added mass coefficient for different order of solution (n). It is obvious that for small values of h/a lower order of solution is reliable but for large values of h/a higher order of solution is required. These figures show that, basically election of $n=4$ is agreeable for whole of quantity of h/a. Performing of the solution until higher order cause that solution procedure be very long. Also, according to Fig. 8, it is clear that with increasing n, the dimensionless added mass increases monotonically.

7) Conclusions

In present paper the analytical solution for the added mass and damping coefficient of a large surface piercing circular cylinder extending to the seabed is prepared. The analytical solution has been obtained by using the eigenfunction expansion procedure. Comparison with previous work indicates good agreement over a range of frequencies the added mass and damping coefficient are plotted along with the actual analytical solutions. Also, influence of solution's order (n) on the final results of added mass coefficient is studied and it could be concluded that for small quantities of h/a lower order of solution is reliable but for large values of h/a higher order of solution is required. Also, these results show that forth order of solution is agreeable generally.

It should be mentioned, in this work because of singular nature of the equation $ka\tanh(kh) = -k_n a\tan(k_n h)$ for a given ka and kh solving procedure is very difficult.

Figure Captions

1. Coordinate system and flow model.

2. Validation of results with the previously published data [15] for dimensionless added damping when $\frac{h}{a} = 3.57.$

3. Validation of results with the previously published data [15] for dimensionless added mass when $\frac{h}{a} = 3.57.$

4. Validation of results with the previously published data [15] for dimensionless added

damping when $\frac{h}{a}=5.0.$

5. Validation of results with the previously published data [15] for dimensionless added mass when $\frac{h}{a}=5.0.$

6. Dimensionless added damping coefficient as a function of ka for various values of $h/a.$

7. Dimensionless added mass coefficient as a function of ka for various values of $h/a.$

8. Analytical solution of added mass coefficient for different order of solution (n) when $\frac{h}{a}=5.0.$

9. Analytical solution of added mass coefficient for different order of solution (n) when $\frac{h}{a}=3.0.$

10. Analytical solution of added mass coefficient for different order of solution (n) when $\frac{h}{a}=1.0.$

11. Analytical solution of added mass coefficient for different order of solution (n) when $\frac{h}{a}=0.5.$

Figures

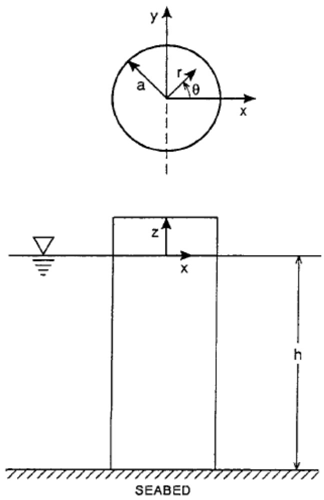

Fig. 1.

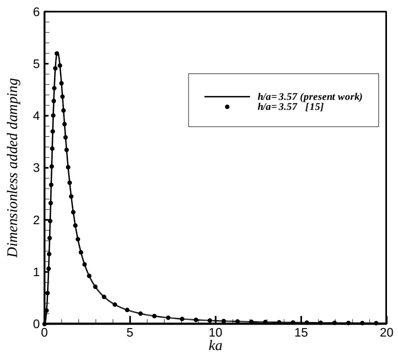

Fig. 2.

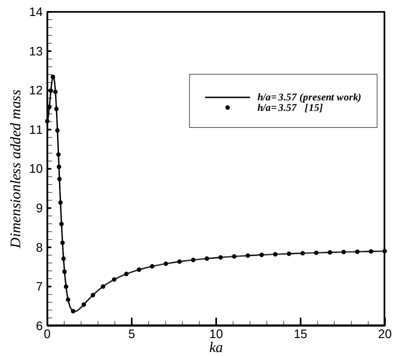

Fig. 3.

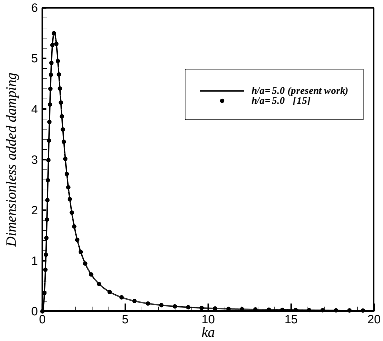

Fig. 4.

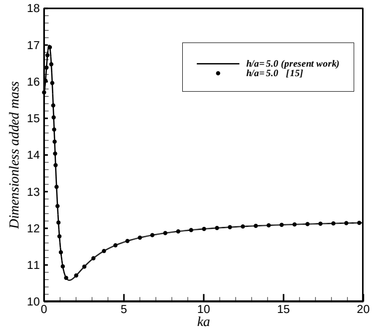

Fig. 5.

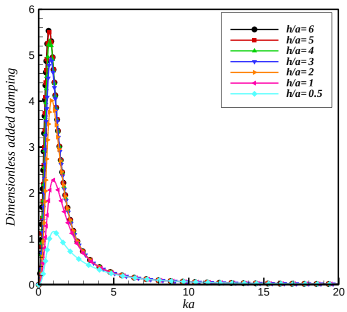

Fig. 6.

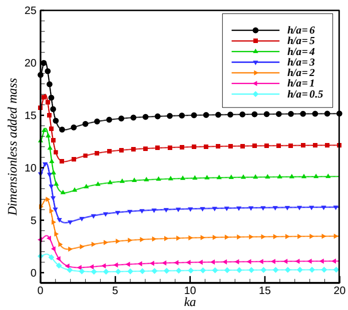

Fig. 7.

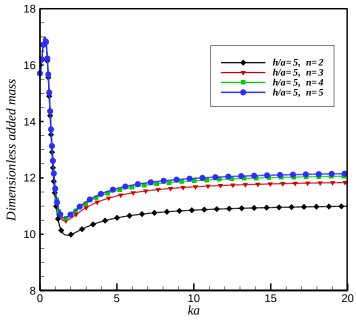

Fig. 8.

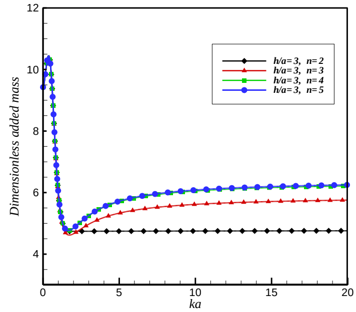

Fig. 9.

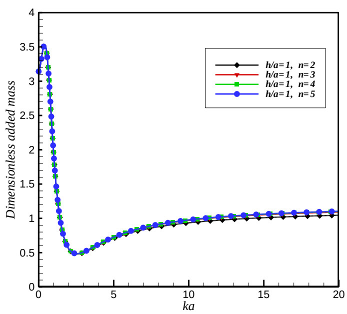

Fig. 10.

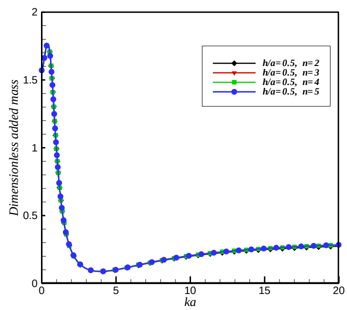

Fig. 11.

Nomenclature

a	radius of circular cylinder
F	force
g	gravitation acceleration
h	depth of water
H_m^1	the m - order Hankel function of the first kind

H_m^2	the m - order Hankel function of the second kind
J_m	the m - order Bessel function of the first kind
k	the wavenumber
K_m	the m - order modified Bessel function of second kind
P	pressure
r	radial distance from the z -axis
t	time
U	complex velocity amplitude
V_n	velocity of the cylinder, normal to surface
x	distance along of wave motion
y	distance perpendicular of wave motion
Y_m	the m - order Bessel function of the second kind
z	vertically upward distance from the still water level
Greek letters	
λ	total added damping
ϕ	complex velocity potential
ω	excitation frequency
η	complex free surface elevation
θ	angular position from the positive x -axis
μ	total added mass
ρ	Water density

References

[1] Sabuncu, T., & Calisal, S. (1981). Hydrodynamic coefficients for vertical circular cylinders at finite depth. *Ocean Engineering*, *8*(1), 25-63. https://doi.org/10.1016/0029-8018(81)90004-4

[2] Pinguet, R., Benoit, M., Molin, B., & Rezende, F. (2022). CFD analysis of added mass, damping and induced flow of isolated and cylinder-mounted heave plates at various submergence depths using an overset mesh method. *Journal of Fluids and Structures*, *109*, 103442. https://doi.org/10.1016/j.jfluidstructs.2021.103442

[3] Yeung, R. W. (1981). Added mass and damping of a vertical cylinder in finite-depth waters. *applied ocean research*, *3*(3), 119-133.https://doi.org/10.1016/0141-1187(81)90101-2

[4] Berhault, C. (1980). An integro-variational method for interior and exterior free surface flow problems. *Applied Ocean Research*, *2*(1), 33-38.https://doi.org/10.1016/0141-1187(80)90045-0

[5] Bai, K. J., Choo, S. M., Chung, S. K., & Kim, D. Y. (2005). Numerical solutions for nonlinear free surface flows by finite element methods. *Applied mathematics and computation*, *163*(2), 941-959. https://doi.org/10.1016/j.amc.2004.04.020

[6] Faltinsen, O. M. (1975). Motions of large structures in waves at zero Froude number. *Norske Veritas*, (90).https://trid.trb.org/View/45816

[7] Fenton, J. D. (1978). Wave forces on vertical bodies of revolution. *Journal of Fluid Mechanics*, *85*(2), 241-255.https://doi.org/10.1017/S0022112078000622

[8] Romano, A., & Bellotti, G. (2023). Wave forces on vertical caissons with retreated wall: A first experimental insight. *Coastal Engineering*, *186*, 104396. https://doi.org/10.1016/j.coastaleng.2023.104396

[9] Chen, H. S., & Mei, C. C. (1976). Oscillations and wave forces in a man-made harbor in the open sea. In *Symposium on Naval Hydrodynamics, 10th, Proceedings, Pap and Discuss, Cambridge, Mass, June 24-28, 1974.* (No. Proceeding).

[10] Rahman, M., & Chakravartty, I. C. (1981). Hydrodynamic loading calculations for offshore structures. *SIAM Journal on Applied Mathematics*, *41*(3), 445-458.http://www.jstor.org/stable/2101451

[11] Rahman, M. (1984). Wave diffraction by large offshore structures: an exact second-order theory. *Applied Ocean Research*, *6*(2), 90-100.https://doi.org/10.1016/0141-1187(84)90046-4

[12] Rahman, M. (1987). A design method of predicting second order wave diffraction caused by large offshore structures. *Ocean engineering*, *14*(1), 1-18. https://doi.org/10.1016/0029-8018(87)90008-4

[13] Drobyshevski, Y. (2004). Hydrodynamic coefficients of a floating, truncated vertical cylinder in shallow water. *Ocean engineering*, *31*(3-4), 269-304.https://doi.org/10.1016/j.oceaneng.2003.07.003

[14] Kazemi, M. A., Jafari, S. S., Musavi, S. M., & Nejati, M. (2018). Analytical solution of convective heat transfer of a quiescent fluid over a nonlinearly stretching surface using Homotopy Analysis Method. *Results in Physics*, *10*, 164-172.https://doi.org/10.1016/j.rinp.2018.05.036

[15] Rahman, M., & Bhatta, D. D. (1993). Evaluation of added mass and damping coefficient of an oscillating circular cylinder. *Applied Mathematical Modelling*, *17*(2), 70-79. https://doi.org/10.1016/0307-904X(93)90095-X

[16] Wu, T. M. (1994). Hydrodynamic loadings acting on submerged bodies advancing in waves—an assessment of accuracy. *Engineering analysis with boundary elements*, *13*(1), 21-33. https://doi.org/10.1016/0955-7997(94)90004-3

[17] Bhatta, D. D. (2007). Computation of added mass and damping coefficients due to a heaving cylinder. *Journal of Applied Mathematics and Computing*, *23*(1), 127-140.https://doi.org/10.1007/BF02831963

[18] Han, R. P. (1996). A simple and accurate added mass model for hydrodynamic fluid—Structure interaction analysis. *Journal of the Franklin Institute*, *333*(6), 929-945. https://doi.org/10.1016/0016-0032(96)00043-9

[19] Boniou, V., Fox, R. O., Posey, J. W., & Houim, R. W. (2024). A multiphase model for fluid–particle flows with added mass and phase change. *Chemical Engineering Journal*, *502*, 157967. https://doi.org/10.1016/j.cej.2024.157967

[20] Sánchez-Caja, A., Martio, J., & Viitanen, V. (2024). On modeling added mass and circulation terms with fast potential-flow methods for oscillating-foil propulsors. *Ocean Engineering*, *313*, 119384. https://doi.org/10.1016/j.oceaneng.2024.119384